Potential Roles of IGF2BP3 in Bladder Cancer

Yu Ye
the First Affiliated Hospital of Guangxi Medical University
Haoxuan Huang
Guangxi Medical University
Rong Huang
the First Affiliated Hospital of Guangxi Medical University
Xi Wang
Guangxi Medical University
Yuanliang Xie
Guangxi Medical University
Caiwang Deng
Guangxi Medical University
Tianyu Li
the First Affiliated Hospital of Guangxi Medical University
Qiuyan Wang
Guangxi Medical University
Zengnan Mo (mozengnan@gxmu.edu.cn)
the First Affiliated Hospital of Guangxi Medical University

Research Article

Keywords: bladder cancer, IGF2BP3

Posted Date: May 19th, 2021

DOI: https://doi.org/10.21203/rs.3.rs-422318/v1

Abstract

The IGF2BP3 can affect cancer cells through the regulation of m6A. In this study, we combined the RNA sequencing and the RNA methylation sequencing to investigate the role and the mechanism of the IGF2BP3 in bladder cancer.TCGA data showed that the intersection genes of RBP differentially expressed and RBP involved in m6A modification were IGF2BP1 and IGF2BP3, only IGF2BP3 was significantly associated with short survival time ($P < 0.01$). Then immunohistochemistry and qRT-PCR detection showed that IGF2BP3 is highly expressed in bladder cancer ($P < 0.05$). The T24 knockout IGF2BP3 cell line was successfully constructed, with cell proliferation decreased and the apoptosis increased ($P < 0.05$). RNA sequencing results of clinical bladder tissue from 53 cases showed that the expression of IGF2BP3 samples were associated with the high levels of proliferation-related genes. The analysis of combined RNA and M6a level showed the differential genes related to cell growth and proliferation: SPHK1, POMT2, MRPS18a in T24 and T24-KO. Our study suggests that the IGF2BP3 is highly expressed in bladder cancer and related to tumor metastasis and invasion, the IGF2BP3 expression is related to cell proliferation genes, which affects the growth, proliferation, and apoptosis of T24 cells, and SpHK1, POMT2, and MRPS18a may be potential targets of IGF2BP3.

Introduction

A total of 2.7 million new patients with bladder cancer are diagnosed or treated in the world every year. Thus, bladder cancer has become the 11th most common cancer worldwide. Bladder cancer has the highest recurrence rate among all malignancies[1,2].

The RNA-binding protein (RBP) regulates the transcriptional and the post-transcriptional levels of most eukaryotic genes and endows each gene with a unique expression profile under specific conditions[3,4]. The insulin-like growth factor-2 (IGF2) messenger RNA (mRNA)-binding protein (IGF2BP) is a kind of mRNA-binding protein (IMP) that regulates the IGF2. The IGF2BP has a high expression in many malignant tumors, such as pancreatic, liver, lung, breast, and colorectal cancers[5-10]. Therefore, the IGF2BP can be used as a valuable tumor marker in human cancer. However, reports show considerable differences in the expression frequency among different types of cancer[11-24], which may be due to the specificity of tissues, use of different antibodies, staining schemes, and scoring standards in experiments. Ramaswamy Suhasini suggest that the IGF2BP3 may promote the expression of the target IGF2 mRNA in an mTOR-controlled manner and promote the tumor's growth [25,26]. Rivera Vargas T et al. have shown that the IGF2BP3 can promote the tumor cells' proliferation through a synergistic effect with HNRNPM in the nucleus, resulting in increased expression of cyclin 9(Rivera Vargas et al., 2014). Furthermore, in triple-negative breast cancer research, the IGF2BP3 can affect the ability of tumor invasion and metastasis[27].

The N6 methyladenosine (m6A) is the most abundant internal modification of mRNA and lncRNA in most eukaryotes and is involved in translation, decay, cell cycle regulation, cell differentiation, and circadian rhythm maintenance[28,29]. The m6A can affect the tumor progression, regulate the RNA stability, and promote the oncogene expression in acute myeloid leukemia, glioblastoma, lung cancer, and liver cancer[30-33].

In this study, we have screened the differentially expressed RBP IGF2BP3 in bladder cancer. The IGF2BP3 is abnormally expressed in clinical bladder cancer tissues. The expression of IGF2BP3 is higher than that in adjacent tissues, whereas no expression in normal bladder tissues is observed. Therefore, we have used biological function experiments and gene sequencing to analyze the role of IGF2BP3 in bladder cancer; explore the primary mechanism of IGF2BP3 in bladder cancer; and provide theoretical bases for early detection, diagnosis, treatment, and monitoring of bladder cancer.

Results

1. RNA-binding proteins analysis reveals an association between IGF2BP3 and bladder cancer by using TCGA database

TCGA data were analyzed, and 206 RBPs with different expressions were selected in accordance with the $|FC|>2$ and the FDR value < 0.05 (Table 1). A total of 29 RBPs were found to be involved in the modification of m6A. The RBP was differentially expressed, and the R package analyzed the RBP involved in the modification of m6A. The overlapping genes were IGF2BP1 and IGF2BP3 (Fig. 1A). The TCGA online data analysis tool GEPIA was used, and the quartile was utilized as the cutoff value to analyze the effect of IGF2BP1 and IGF2BP3 expression on the survival time of patients with bladder cancer. The survival analysis showed that the survival time of patients with high expression of IGF2BP3 was significant shorter than that of patients with low expression of IGF2BP3. By contrast, the expression of IGF2BP1 had no significant relationship with the survival time of patients (Fig. 1B).

Table 1: Correlation between differentially expressed RBPs and survival analysis

RBP	log2FC	FDR	Hazard Ratio	P-value
AHNAK	−1.4764504	4.29E−10	1.009636108	3.93E−08
RBMS3	−2.57621295	3.77E−17	1.10784303	9.46E−05
MAP1B	−2.97123858	1.42E−21	1.045547367	0.000104752
P4HB	1.13242358	7.89E−11	1.000852667	0.00014117
VIM	−1.38494732	7.81E−06	1.000351378	0.000162224
LIN28B	1.853549784	0.042039466	1.230186446	0.000256573
ATXN1	−1.33445898	7.40E−07	1.068881358	0.000381688
LRP1	−1.08109479	3.27E−05	1.008057353	0.000748507
TRIM71	1.373495559	0.004815579	1.274966945	0.000801275
IGF2BP1	3.539824148	0.000526821	No	No
IGF2BP3	3.200017062	0.018016805	1.042559323	0.00116792

2. The high expression of IGF2BP3 in bladder cancer tissue was compared with its clinicopathological characteristics in clinical sample

Combined with the pathological information, immunohistochemistry showed that the overall positive rate of 72 cases of bladder cancer was 44.4% (32/72) (Fig. 1B). Statistical analysis showed that the expression of IGF2BP3 in bladder cancer was different: 11% (8/72) of the patients were strongly positive (+++), 33.3% (24/72) were positive staining (+, ++), 55.6% (40/72) were occasional focal staining or no staining; and 12 cases of normal bladder tissue sections were not observed with stained areas (cells). The positive rate of the IGF2BP3 expression in bladder cancer tissues was significantly higher than that in normal tissues (Table 2).

Table 2 Comparison of IGF2BP3 expression in bladder cancer and normal bladder tissue

Bladder tissue	Patient Number	+	-	P-value
Cancer	72	32	40	<0.01
Normal	12	0	12	<0.01

The clinicopathological characteristics of 72 cases of positive rate of bladder cancer were as follows: (1) pathological classification: positive rate of 68 urothelial carcinoma samples was44.1% (30/68); (2) gender ratio: positive rate of 62 male patients samples was 45.2% (28/62), positive rate of 11 female patients samples was 36.4% (4/11); (3) pathological grade: positive rate of 67 high-grade samples samples was 44.8% (30/67), positive rate of 5 low-grade samples was 40% (2/5); (4) TNM: positive rate of 11 patients with tumor staging below T1 was 45.5% (5/11), and that of 61 patients over T2 stage was 44.3% (27/61)44.3% (27/61); (5) infiltration: positive rate of 59 invasive samples was 50.8%, positive rate of 13 noninvasive samples was 15.4% (2/13); (6) metastasis: positive rate of 14 lymph node metastasis samples= 71.4% (10/14), positive rate of 58 Patients without lymph node metastasis was37.9% (22/58). The IGF2BP3 expression had no significant correlation with gender, age, pathological grade, and T stage, but the positive rate was high in lymph node metastasis and tumor invasion samples ($P < 0.05$) (Table 3).

Table3 Comparison of the positive rates of IGF2BP3 in bladder cancer tissues between clinicopathological characteristics of patients

Patient features	Group	Number	+	-	P-value
Age	<65	37	16	21	>0.05
	≥65	35	16	19	
Gender	Male	61	28	33	>0.05
	Female	11	4	7	
Grades	High	67	30	37	>0.05
	Low	5	2	3	
Clinical T stages	≤T1	11	5	6	>0.05
	≥T2	61	27	34	
Lymph node metastasis	Yes	14	10	4	<0.05
	No	58	22	36	
Invasion	Yes	59	30	29	<0.05
	No	13	2	11	

The qRT-PCR was used to detect the relative expression of IGF2BP3 in 27 pairs of clinical bladder cancer and corresponding paracancerous tissues. Results showed that the expression of IGF2BP3 in cancer tissues (C.A. blue) was higher than that in paracancerous tissues (C.P. red),

and the difference was statistically significant ($P < 0.05$, Fig. 2B).

3. Construction of the CRISPR/cas9 recombinant vector and T24 cells with knockout IGF2BP3

To further explore the effect of IGF2BP3 on bladder cancer cells, we constructed T24 cells with knockout IGF2BP3. The expression of the IGF2BP3 in SW780, J82, 5637, and T24 bladder cancer cell lines was detected using Western blot. The IGF2BP3 was highly expressed in 5637 and T24 cells (Fig. 3A). In view of the easy transfection of T24 cells, subsequent knockout experiments were carried out in T24 cells. After cutting the bsmbi site on the vector (Fig. 3B), the plasmid DNA was extracted and sequenced. Results showed that at the RNA level, the construction of the vector was successful (Fig. 3C). The lentiviral vector plasmid was injected into the cells, and DNA amplification was sent to the company for sequencing, which showed a base mutation in the sequence near the knockout site (Fig. 3D). Results showed that at the protein level, compared with control cells, ko#3 cells almost did not express the IGF2BP3, which proved that ko#3 cells successfully knocked out the IGF2BP3 gene (Fig. 3E).

4. The biological function detect of T24 and IGF2BP3 T24–KO cells

Next, we tested the biological function of knockout T24 cells. The clone numbers of T24 and IGF2BP3 T24–KO cells were 152 ± 17 and 108 ± 16, respectively. According to the SPSS, a significant difference in colony-forming ability was observed between T24 and T24–KO cell lines ($P < 0.001$, Fig.4A). After the cells were seeded into 96-well plates, the cell proliferation activity was measured at 12, 24, 36, 48, and 72 h. On the second day, the proliferation ability of T24–KO cells was significantly lower than that of T24 cells (Fig. 4B). The apoptosis rates of T24 and T24–KO cells were detected using flow cytometry. Compared with that of T24 cells, the apoptosis of T24–KO cells was significantly increased ($P < 0.01$, Fig. 4C). The migration distance between T24–KO and T24 cells was observed under the microscope for 0 and 24 h. Results showed no significant change in the migration distance between T24–KO and T24 cells (Fig. 4D). After 24 h, the transwell chamber was obtained for staining, and the number of invasive cells was calculated by randomly observing five fields under the microscope. No significant difference was observed in the number of invasive cells between T24–KO and T24 cells (Fig. 4E).

5. IGF2BP3 was highly expressed associated with cell proliferation markers in clinical bladder cancer tissues

To further explore the mechanism of IGF2BP3 in clinical bladder cancer, We further further performed RNA sequencing on 53 clinical bladder tissues. The samples were first arranged according to the expression of IGF2BP3, and the samples were grouped according to the molecular subtypes, then, the characteristic gene expression was clustered using the R software (Fig 5A-B). Results showed no significant correlation between the expression level of IGF2BP3 and the six subtypes of bladder cancer (Fig. 5A). Compared with the low expression of IGF2BP3, the expression of molecular markers related to cell proliferation was higher in tissues with high expression of IGF2BP3 (Fig. 5B). Also, the expression of some genes related to EMT increased (Fig. 5C).

6. Analysis of differences in RNA levels between T24 and IGF2BP3 T24–KO cells

The downstream pathway of IGF2BP3 was further analyzed by sequencing data. According to the list of expressed genes, the gene expression value of 0 was eliminated. A total of 1149 genes were screened in accordance with the fold change $|FC| \geq 1.5$ and adj. $P < 0.05$. A total of 847 genes were upregulated, and 302 genes were downregulated. The GO analysis showed five pathways with abundant differential genes in BP (i.e., extracellular matrix organization, positive regulation of cell adhesion, extracellular structure organization, positive regulation of vascular development, and regulation of trans-synthetic signaling), CC (i.e., collagen-containing extracellular matrix, cell–cell junction, membrane raft, membrane microdomain, and membrane region), and MF (i.e., receptor–ligand activity, receptor–ligand activity, glycosaminoglycan binding, heparin binding, and growth factor receptor binding; Fig. 6A). The most significantly enriched KEGG pathway genes were TNF signaling pathway, AGE–RAGE signaling pathway in diabetic complexes, rheumatoid arthritis, and MAPK signaling pathway (Fig. 6B).

7. m6A and RNA sequencing were combined to analyze T24 and IGF2BP3 T24–KO cells

We combined RNA and m6A data for further comparison. The quality control of m6A data was qualified (Table 4). The genome distribution of the m6A peak was found using the IGF2BP3 motif (GGAC). No significant difference was observed between T24 and T24–KO cells (Fig. 7A). The related genes with m6A modification were counted and compared between T24 and T24–KO groups. GO and KEGG databases were used for the enrichment analysis. The top 10 pathways enriched in GO analysis were related to gene transcription regulation, chromosome modification, and RNA splicing (Fig. 7B); and the top five pathways enriched in KEGG analysis were Hippo signaling pathway, protein processing in the endoplasmic reticulum, neurotrophin signaling pathway, renal cell carcinoma, and insulin signaling pathway (Fig. 7C). The intersection of genes with different m6A levels ($|FC| > 2$, $P < 0.05$) and different transcription expression levels ($|FC| > 1$, $P < 0.05$) was obtained (Fig. 7D), and the 4-quadrant diagram of genes with the intersection part (Fig. 7E) was demonstrated on the basis of the transcriptome sequencing. Results showed that the genes WDR6, SPHK1, MRPS18A, POMT2, UBE2G1, SAV1, MAP3K5, AJUBA, and FAM213

changed in gene expression and m6A level. TCGA was used to analyze the correlation of WDR6, SPHK1, MRPS18A, POMT2, FAM213A, and IGF2BP3 expression levels (Fig. 7F) with the expression differences in clinical samples (Fig. 7G). Results suggested that the expression levels of SPHK1, POMT2, and MRPS18A were positively correlated with the IGF2BP3. The expression level of cancer was higher than that of normal tissue and was consistent with our sequencing results. After the IGF2BP3 knockout, the expression levels of SPHK1, POMT2, MRPS18A, and m6A in T24 cells decreased.

Table 4 Quality control table for MeRIP-seq samples

SampleName	Encoding	TotalReads (Before)	TotalBase_ (Before)	TotalReads_ (After)	TotalBase_ (After)	ReadsFilter%	BaseFilter%	GC%_ (Before)	GC%_ (After)
T24-1-input	Sanger / Illumina 1.9	41910989	6.29E+09	38644728	5.23E+09	0.922067	0.831496567	59	59
T24-1-IP	Sanger / Illumina 1.9	49523858	7.43E+09	45586431	6.56E+09	0.920494	0.883250188	57	57
T24-2-input	Sanger / Illumina 1.9	40791901	6.12E+09	36880837	5.07E+09	0.904122	0.82932371	58	59
T24-2-IP	Sanger / Illumina 1.9	45352767	6.8E+09	42095946	6.04E+09	0.928189	0.88771009	55	56
ko1-input	Sanger / Illumina 1.9	40834445	6.13E+09	35883952	4.84E+09	0.878767	0.790551884	58	58
ko1-IP	Sanger / Illumina 1.9	52956267	7.94E+09	47625102	6.83E+09	0.899329	0.860200677	52	53
ko2-input	Sanger / Illumina 1.9	38380741	5.76E+09	36074398	5.14E+09	0.939909	0.89307513	60	60
ko2-IP	Sanger / Illumina 1.9	41372245	6.21E+09	38398666	5.52E+09	0.928126	0.890101522	53	54

Discussion

The IGF2BP3 is initially identified as a highly overexpressed gene in pancreatic cancer. Subsequently, increasing evidence shows that the IGF2BP3 is abnormally expressed in various tumor tissues and affects patients' survival and prognosis in varying degrees[34]. The IGF2BP3 is not expressed in benign, low-grade, and high-grade noninvasive urothelial carcinomas[35]. The expression levels of IGF2BP3 are 11.76% and 55% in low- and high-grade invasive urothelial carcinomas, respectively. Compared with that in noninvasive specimens, the expression of the IGF2BP3 in invasive urothelial carcinoma is statistically significant ($P < 0.000$). This result suggests that the expression of the IGF2BP3 is related to the invasion of bladder cancer. Another study found that, the 5-year progression-free and disease-free survival rates for IGF2BP3 negative patients were 91% and 94%, while those of IGF2BP3 positive patients were 64% and 76%. [36]. In patients with superficial invasive urothelial carcinoma, IGF2BP3 positive patients are more likely to have metastasis than IGF2BP3 negative patients ($P = 0.0017$).

The bladder urothelial carcinoma is usually divided into nonmuscle- and muscle-invasive urothelial carcinomas. Given the hospital treatment plan factors, patients with nonmuscle invasive bladder cancer are generally treated by the transurethral resection of the bladder tumor, and the resection of the tissue is small. Thus, this part of specimens is difficult to collect. Patients with muscle-invasive bladder cancer are often treated with cystectomy. The removed tissue is large and comfortable to collect. Therefore, most of the specimens we have collected are muscle-invasive urothelial carcinoma; a few are nonmuscle invasive urothelial carcinoma; and some are adenocarcinoma, squamous cell carcinoma, and neuroendocrine carcinoma. Immunohistochemical experiments are carried out on the collected clinical tissues to verify the expression level of IGF2BP3 in clinical samples in TCGA database. Results show the abnormal expression of the IGF2BP3 gene in bladder cancer tissues and almost no expression in normal tissues ($P < 0.01$). At the same time, the expression level of the IGF2BP3 is detected in

bladder cancer and corresponding adjacent tissues by qRT-PCR, and these results are consistent with those of immunohistochemistry. qRT-PCR results show that the expression level of IGF2BP3 in cancer tissues is higher than that in adjacent tissues ($P < 0.05$). Clinical and pathological data show that the positive rate of the IGF2BP3 is higher in lymph node metastasis and invasive specimens ($P < 0.01$). However, due to small sample size, the relationship among the IGF2BP3, lymph node metastasis, and bladder cancer invasion should be further proven. The survival and the prognosis of IGF2BP3 patients are difficult to analyze because of incomplete collection of clinical samples and pathological data. Also, the expression of the IGF2BP3 in nonmuscle invasive urothelial carcinoma is significantly correlated with advanced tumor stage ($P < 0.001$), advanced tumor grade ($P = 0.004$), and tumor recurrence ($P < 0.001$)[37]. The IGF2BP3 expression in the nonmuscle invasive urothelial carcinoma is an independent unfavorable prognostic factor for disease-free survival. Given that most of the specimens we have collected are muscle-invasive bladder cancer, the expression of the IGF2BP3 in the nonmuscle invasive urothelial cancer and its impact on survival and prognosis should be increased in the future. After the expression of the IGF2BP3 in clinical tissues is verified, the biological function of the IGF2BP3 in bladder cancer cells should be further studied. Considering the increased expression of the IGF2BP3 in bladder cancer to facilitate the stability of subsequent cell experiments, the CRISPR/cas9 system is used to construct stable cell lines with the IGF2BP3 knockout.

The CRISPR/cas9 technology is recognized as a potentially transformative application in transcriptional interference, epigenetic regulation, base editing, high-throughput genetic screening, and animal or cell models of diseases[38]. Compared with ZFN and talen, the CRISPR/cas9 technology is convenient, economical, and efficient. This study has used the CRISPR/cas9 system to knock out the IGF2BP3 gene in the human bladder cancer cell line T24. After the knockout, the DNA sequencing shows that the gene sequence has a base mismatch and that the target sequence has an overlapping peak. This finding may be due to the tetraploid T24 cells and different base repairs after the gene knockout. Finally, the Western blot confirms that the knockout cell line almost does not express the IGF2BP3 protein, indicating that the gene knockout is successful.

The IGF2BP3 (IMP3) gene is an IGF2. Members of the IMP family play an essential role in the early development of the embryo, neuron, and reproductive system. As RBP, the IMP can affect the growth, proliferation, cell cycle, migration, and invasion of cancer cells by regulating the transport, translation, modification, and stability of the RNA. The IGF2BP3 gene can directly regulate tumor cells. Huang et al. have found that the proportions of IGF2BP3 and CD44 + CD24−ESA + cell clusters in the silenced mammary sum315 cell line are significantly decreased, and their spheroidizing ability is significantly inhibited. After the re-expression of the IGF2BP3, the self-renewal ability and the tumorigenic potential of the sum315 are restored[39]. Zhao et al. have silenced the expression of the IGF2BP3 in lung cancer A549 cell line by shRNA and found that the ability of cell proliferation and tumor migration and invasion are significantly decreased, whereas the overexpression of IGF2BP3 significantly promotes cell proliferation and tumor migration and invasion[40]. You et al. observed that silencing IGF2BP3 gene of SW620 and SW480 resulted in decreased proliferation activity, increased apoptosis and decreased invasion ability of cells. [41]. In the present study, functional experiments are performed on T24 bladder cancer cells with the IGF2BP3 knockout. Differences in proliferation, colony formation, apoptosis, migration, and invasion between the knockout and the control cells are determined. Results show differences in cell proliferation, colony-forming ability, and apoptosis ($P < 0.05$). However, the scratch and the transwell invasion tests show that the cell migration and invasion abilities do not change significantly. This phenomenon may be related to the characteristics of cell lines. Various cell lines should be selected to analyze cell biological function changes comprehensively and verify the cell function.

The IGF2BP3 gene plays a vital role in many tumors. In tumor development, the IGF2BP3 has shown the role of promoting cancer by influencing the tumor cell proliferation, apoptosis, migration, invasion, and drug resistance. The abnormal expression of IGF2BP3 in bladder tumors is determined in the first part of this study. The IGF2BP3 knockout T24 cell line is constructed, the verification of the cell biological function showed that the IGF2BP3 was associated with cell population dependence, proliferation, and apoptosis. In the second part of the study, the RNA sequencing is used to analyze the expression and the significance of the IGF2BP3 in clinical tissue samples. Given the increase in the IGF2BP3 expression, the expression of proliferation-related genes, such as ANLN, ASF1B, CCNB1, and CCNA2, also increases. Only SNAI2, CCN4, and FAP are consistent with the expression of the IGF2BP3. This result is consistent with our cell experiment. Finally, the RNA sequencing and the m6A methylation sequencing of cell samples are performed. Some differences are observed between T24 and T24–KO in the transcriptome, m6A-modified gene sets, and GO and KEGG enrichment analysis pathways. At the transcriptional level, the differentially expressed genes in the knockout and the control groups are related to cell growth, differentiation, development, cancer, inflammation, and other related pathways. At the m6A modification level, the differentially expressed genes are related to cell growth, endoplasmic reticulum protein processing, splicing, cancer, and other related pathways. These results suggest that the IGF2BP3 may regulate the cell biological function in different ways at the transcription and the m6A levels. The essential genes involved in these two regulatory pathways are significant. After crossing the differential genes of the two groups and the differential genes of m6A, there were 191 genes significantly different at RNA and M6a levels. The IGF2BP3 is considered a protein that recognizes and binds to the mRNA modified by m6A, which can stabilize the target mRNA and promote translation. WDR6, sphingosine kinase (SPHK) 1, MRPS18A, POMT2, and FAM213A, whose expression level is consistent with IGF2BP3, are selected, and their correlation with IGF2BP3 expression tissues is analyzed in TCGA database

online analysis tool GEPIA. Results show that SPHK1, MRPS18A, and POMT2 are positively correlated with IGF2BP3, and the expression levels of SPHK1, MRPS18A, and POMT2 in carcinoma are higher than those in normal tissues. The sphingosine-1-phosphate (S1P), a bioactive metabolite of sphingosine, is associated with tumor progression by enhancing the cell proliferation and motility. The SPHK can catalyze the formation of S1P, regulate sphingolipid rheostat, and promote tumor growth in various cancers. Related studies have shown that the increased expression of SPHK1 can promote tumor cell growth by increasing a variety of carcinogenic processes, including proliferation and self-renewal in vitro and tumor growth in vivo[42-44]. The POMT2 plays a crucial role in embryogenesis and development. Some studies have shown that the POMT2 can change the expression of E-cadherin, the essential protein involved in cell adhesion[45]. The increased expression of MRPS18A in human breast cancer cells can be explained by the increased energy metabolism of cancer cells, which indicates that MRPS18A may be involved in tumorigenesis[46]. In conclusion, after the IGF2BP3 knockout in T24 cells, the level and the m6A expression of SPHK1, MRPS18A, and POMT2 genes are downregulated and may be the target genes of IGF2BP3.

In this study, we showed that the IGF2BP3 was highly expressed in bladder cancer tissue and cell lines. This finding was related to tumor metastasis and invasion and growth, proliferation, and apoptosis of T24 cells. We mainly revealed that SPHK1, POMT2, and MRPS18a might be potential targets of IGF2BP3 in T24 cells at RNA and m6A levels by sequencing, This result needs to be verified in the next project, but it provides valuable research ideas for further research.

Methods

1. Clinical samples and cell lines

A total of 72 pairs of fresh BCa and adjacent tissue specimens were obtained from the First Affiliated Hospital of Guangxi Medical University from September 2015 to September 2019. Institutional review board approval was obtained from GXMU for the collection of BCa and adjacent tissue and written informed consent was obtained from all patients. Cell lines T24, 5637, SW780, and J82 were obtained from the Cell Bank, Chinese Academy of Sciences (Shanghai, China) . All methods were performed in accordance with the relevant guidelines and regulations.

2. Cell culture

Cells were maintained in the RPMI-1640 medium (HyClone, USA) supplemented with 10% fetal bovine serum (HyClone, USA) and 1% penicillin–streptomycin solution (HyClone, USA) and grown in an incubator maintained at 37 °C and 5% CO2.

3. RNA extraction and qRT-PCR

The total RNA was extracted in accordance with the instructions in the Magen's total RNA extraction kit. The mRNA expression level was detected, and mRNAs were reversely transcribed into cDNA by using the PrimeScript™ RT reagent kit (TaKaRa). The PCR amplification was performed using the SYBR Premix Ex Taq™ (TaKaRa) in the Real-Time PCR System (Bio-Rad, USA). The 2−ΔΔCt method was used to calculate the relative miRNA expression.

4. CRISPR/Cas9-mediated genome editing of the knockout IGF2BP3 in the bladder cell

The IGF2BP3–gRNA vector was constructed by Jiman Biotechnology Co., Ltd(Shanghai, China). Primer-F (5' to 3') CACCGAGGCGCAGAGGCAAATCACA and Primer-R (5' to 3') AAACTGTGATTTGCCTCTGCGCCTC were subcloned into the lentiviral vector (Fig. 2A). Cloning was performed in accordance with the standard protocols in HEK 293T cells. Lentiviral particles transduced immortalized human podocytes, and single-cell clones of CRISPR/Cas9 genome-edited podocytes were generated. The DNA sequencing and the Western blot analysis were used to to verify the establishment of t24-ko cells.

5. Immunohistochemistry

Tissues were collected within 30 min after tumor resection and fixed in formalin for 48 h. The sections were incubated with primary antibodies at 4 °C overnight (Abcam, USA). The corresponding secondary antibodies conjugated to horseradish peroxidase were incubated with the sections for 1 h at room temperature. After washing with PBS, the sections were reacted with diaminobenzidine prior to counterstaining with hematoxylin. Images were acquired using the Leica Microsystems (Leica, Germany).

6. Western blot analysis

Tissues and cells were lysed in RIPA buffer (Boster, China). Lysates were denatured at 95 °C for 5 min and cooled using ice. Lysates were loaded onto the sodium dodecyl sulfate–polyacrylamide gel (10% SDS–PAGE) and electrotransferred onto the polyvinylidene difluoride (PVDF) membrane. PVDF membranes were blotted with the primary antibody at 4 °C for 12 h and incubated with HRP-labeled secondary

antibody (Invitrogen, USA) at room temperature for 2 h. The primary antibodies were as follows: rabbit monoclonal antibody to IGF2BP3 (Abcam, USA), mouse monoclonal antibody to GAPDH (Abcam, USA), and rabbit monoclonal antibody to β-actin (Abcam, USA).

7. Colony formation, MTT, flow cytometry, scratch, and transwell cell invasion analyses

Cells were seeded into 6-well plates and grown for 10 days. Visible colonies (≥ 50 cells) were counted after methanol fixation and Giemsa staining. After transfection, cells were cultured into 96-well plates with 1000 cells/well. Each well was added with MTT solution and incubated at 37 °C for another 4 h. The medium was collected, and 100μl DMSO was added into each well. The microplate reader was used to detect the absorbance of the plate (490 nm). Cells were stained with annexin V–FITC and PI (BestBio, China) and analyzed using flow cytometry (BD. Biosciences). Apoptotic cells were detected and analyzed using the CellQuest software (BD. Biosciences). Only the early apoptosis rates of cells were determined to analyze the results. Approximately 3×106 cells were evenly spread, and the cell layer was carefully scratched with a sterile tip. Cells were incubated for 0 and 24 h, and a 24-well plate transwell chamber system (Corning, USA) was used to acquire images. Membrane cells were fixed in 4% PFA for 15 min and stained with 0.1% Gimsa for 20 min. The stained chambers were left to dry and photographed. All experiments were repeated thrice.

8. RNA-seq and MeRIP-seq

For the RNA-seq, the total RNA was first extracted from T24 with the stable IGF2BP3 knockout and sent to Mingma Technology Co., Ltd. (Shanghai, China). The Fastqc was used for the quality control of sequencing data, and the Hisat2 software was used for sequence alignment. The Samtool and the Stringtie were used to convert the data format and assemble the transcript. The DESeq2 was used for differential expression analysis, and the absolute value of FoldChange (FC) ≥ 1.5 and adjusted P ≤ 0.05 were set as the cutoff criteria. The Gene Ontology (GO) functional annotation and the gene pathway (KEGG) analyses were used for further study. For the MeRIP-seq, after sending the cell samples to Guangzhou Epi-Biotech Co., Ltd. (Guangzhou, China), the total RNA extraction, RNA fragmentation, methylated RNA enrichment, methylated RNA recovery, sequencing library construction, sequencing, and data quality control were performed. The analysis process included peak calling statistics, peak annotation, motif analysis, and differential peak analysis. The correlation analysis was used to analyze the differential genes of m6A and differential expression genes and visualize GO and KEGG analyses.

9. Statistical analysis

Statistical analyses were performed using the IBM SPSS v17.0 (IBM Co., Armonk, NY, USA). The relationship between IGF2BP3 expression in normal tissues and pathological features of bladder cancer was analyzed by chi square test and Fisher's exact test. The RNA expression level of IGF2BP3 in corresponding paracancerous tissues of bladder cancer was compared by chi square test and one-way ANOVA. All data were expressed as mean ± standard deviation (n ≥ 3). P < 0.05 was considered statistically significant..

Declarations

Declaration of competing interest

The authors declare no competing financial interest.

Author Contribution statement

Yu Ye: Experimental operation. **Haoxuan Huang:** Experimental operation. **RongHuang:** Article writing. **WangXi:** Data analysis. **Yuanliang Xie:** Specimen collection. **Caiwang Deng:** Experimental operation. **Tianyu Li:** Specimen collection. **Qiuyan Wang:** Guidance of project ideas. **Zengnan Mo:** The project bears the responsibility.

References

1 Grayson, M. Bladder cancer. *Nature* **551**, S33, doi:10.1038/551S33a (2017).

2 Lenfant, L., Aminsharifi, A., Seisen, T. & Roupret, M. Current status and future directions of the use of novel immunotherapeutic agents in bladder cancer. *Curr Opin Urol* **30**, 428-440, doi:10.1097/MOU.0000000000000740 (2020).

3 Orphanides, G. & Reinberg, D. A unified theory of gene expression. *Cell* **108**, 439-451, doi:10.1016/s0092-8674(02)00655-4 (2002).

4 Chen, K. & Rajewsky, N. The evolution of gene regulation by transcription factors and microRNAs. *Nat Rev Genet* **8**, 93-103, doi:10.1038/nrg1990 (2007).

5 Hammerle, M. *et al.* Posttranscriptional destabilization of the liver-specific long noncoding RNA HULC by the IGF2 mRNA-binding protein 1 (IGF2BP1). *Hepatology* **58**, 1703-1712, doi:10.1002/hep.26537 (2013).

6 Nguyen, L. H. *et al.* Lin28b is sufficient to drive liver cancer and necessary for its maintenance in murine models. *Cancer Cell* **26**, 248-261, doi:10.1016/j.ccr.2014.06.018 (2014).

7 Chatterji, P. & Rustgi, A. K. RNA Binding Proteins in Intestinal Epithelial Biology and Colorectal Cancer. *Trends Mol Med* **24**, 490-506, doi:10.1016/j.molmed.2018.03.008 (2018).

8 Cui, X. H., Hu, S. Y., Zhu, C. F. & Qin, X. H. Expression and prognostic analyses of the insulin-like growth factor 2 mRNA binding protein family in human pancreatic cancer. *BMC Cancer* **20**, 1160, doi:10.1186/s12885-020-07590-x (2020).

9 Ma, F. *et al.* Long non-coding RNA FGF13-AS1 inhibits glycolysis and stemness properties of breast cancer cells through FGF13-AS1/IGF2BPs/Myc feedback loop. *Cancer Lett* **450**, 63-75, doi:10.1016/j.canlet.2019.02.008 (2019).

10 He, Y. *et al.* Long noncoding RNAs: Novel insights into hepatocelluar carcinoma. *Cancer Lett* **344**, 20-27, doi:10.1016/j.canlet.2013.10.021 (2014).

11 Mentrikoski, M. J. *et al.* Diagnostic utility of IMP3 in segregating metastatic melanoma from benign nevi in lymph nodes. *Mod Pathol* **22**, 1582-1587, doi:10.1038/modpathol.2009.128 (2009).

12 Walter, O. *et al.* IMP3 is a novel biomarker for triple negative invasive mammary carcinoma associated with a more aggressive phenotype. *Hum Pathol* **40**, 1528-1533, doi:10.1016/j.humpath.2009.05.005 (2009).

13 Wang, B. J., Wang, L., Yang, S. Y. & Liu, Z. J. Expression and clinical significance of IMP3 in microdissected premalignant and malignant pancreatic lesions. *Clin Transl Oncol* **17**, 215-222, doi:10.1007/s12094-014-1216-4 (2015).

14 Feng, W. *et al.* Expression of insulin-like growth factor II mRNA-binding protein 3 in human esophageal adenocarcinoma and its precursor lesions. *Arch Pathol Lab Med* **135**, 1024-1031, doi:10.5858/2009-0617-OAR2 (2011).

15 Fadare, O. *et al.* Expression of the oncofetal protein IGF2BP3 in endometrial clear cell carcinoma: assessment of frequency and significance. *Hum Pathol* **44**, 1508-1515, doi:10.1016/j.humpath.2012.12.003 (2013).

16 Vercellini, P. *et al.* The oncofetal protein IMP3: a novel biomarker and triage tool for premalignant atypical endometriotic lesions. *Fertil Steril* **99**, 1974-1979, doi:10.1016/j.fertnstert.2013.02.002 (2013).

17 Wei, Q., Fu, B., Liu, J., Xu, J. & Zhao, T. Combined detection of p16(INK4a) and IMP3 increase the concordance rate between cervical cytologic and histologic diagnosis. *Int J Clin Exp Pathol* **6**, 1549-1557 (2013).

18 Lastra, R. R. *et al.* Utility of ProExC and IMP3 immunocytochemical staining in atypical glandular cells of undetermined significance in liquid-based cervical cytology. *Diagn Cytopathol* **42**, 375-379, doi:10.1002/dc.23029 (2014).

19 Su P, Hu J & Zhang H, e. a. IMP3 expression is associated with epithelial-mesenchymal transition in breast cancer. *Int J Clin Exp Pathol* **7**, 3008-3017 (2014).

20 Trivedi, A., Cartun, R. W. & Ligato, S. Role of lymphovascular invasion and immunohistochemical expression of IMP3 in the risk stratification of superficially invasive pT1 esophageal adenocarcinoma. *Pathol Res Pract* **210**, 402-406, doi:10.1016/j.prp.2014.01.018 (2014).

21 Wang, L., Li, H. G., Xia, Z. S., Lu, J. & Peng, T. S. IMP3 is a novel biomarker to predict metastasis and prognosis of gastric adenocarcinoma: a retrospective study. *Chin Med J (Engl)* **123**, 3554-3558 (2010).

22 Palanichamy, J. K. *et al.* RNA-binding protein IGF2BP3 targeting of oncogenic transcripts promotes hematopoietic progenitor proliferation. *J Clin Invest* **126**, 1495-1511, doi:10.1172/JCI80046 (2016).

23 Gadara, M. R., Gonzalez, M., Cartun, R. W. & Ligato, S. IMP3 Immunoreactivity is More Sensitive Than AMACR in Detecting Dysplastic Epithelium and Early Adenocarcinoma in Barrett Esophagus. *Appl Immunohistochem Mol Morphol* **25**, 386-391, doi:10.1097/PAI.0000000000000319 (2017).

24 Seo, J. W., Ha, S. M. & Song, K. H. Insulin-like growth factor-2 mRNA-binding protein 3 as a novel prognostic biomarker for acral lentiginous melanoma. *Br J Dermatol* **178**, e268-e270, doi:10.1111/bjd.16077 (2018).

25 Liao, B., Hu, Y., Herrick, D. J. & Brewer, G. The RNA-binding protein IMP-3 is a translational activator of insulin-like growth factor II leader-3 mRNA during proliferation of human K562 leukemia cells. *J Biol Chem* **280**, 18517-18524, doi:10.1074/jbc.M500270200 (2005).

26 Suvasini, R. *et al.* Insulin growth factor-2 binding protein 3 (IGF2BP3) is a glioblastoma-specific marker that activates phosphatidylinositol 3-kinase/mitogen-activated protein kinase (PI3K/MAPK) pathways by modulating IGF-2. *J Biol Chem* **286**, 25882-25890, doi:10.1074/jbc.M110.178012 (2011).

27 Gao, Y. *et al.* IMP3 expression is associated with poor outcome and epigenetic deregulation in intrahepatic cholangiocarcinoma. *Hum Pathol* **45**, 1184-1191, doi:10.1016/j.humpath.2014.01.016 (2014).

28 Chen, Y. L. *et al.* Expression of insulin-like growth factor II mRNA-binding protein 3 predicts early recurrence and poor prognosis in intrahepatic cholangiocarcinoma. *Int J Surg* **11**, 85-91, doi:10.1016/j.ijsu.2012.11.021 (2013).

29 Hu, S. *et al.* IMP3 combined with CD44s, a novel predictor for prognosis of patients with hepatocellular carcinoma. *J Cancer Res Clin Oncol* **140**, 883-893, doi:10.1007/s00432-014-1639-x (2014).

30 Huang, Y. *et al.* Small-Molecule Targeting of Oncogenic FTO Demethylase in Acute Myeloid Leukemia. *Cancer Cell* **35**, 677-691 e610, doi:10.1016/j.ccell.2019.03.006 (2019).

31 Dong, Z. & Cui, H. The Emerging Roles of RNA Modifications in Glioblastoma. *Cancers (Basel)* **12**, doi:10.3390/cancers12030736 (2020).

32 Zhang, C. *et al.* YTHDF2 promotes the liver cancer stem cell phenotype and cancer metastasis by regulating OCT4 expression via m6A RNA methylation. *Oncogene* **39**, 4507-4518, doi:10.1038/s41388-020-1303-7 (2020).

33 Zhang, Y. *et al.* Expression and Prognostic Significance of m6A-Related Genes in Lung Adenocarcinoma. *Med Sci Monit* **26**, e919644, doi:10.12659/MSM.919644 (2020).

34 Jiang, Z. *et al.* Analysis of RNA-binding protein IMP3 to predict metastasis and prognosis of renal-cell carcinoma: a retrospective study. *Lancet Oncol* **7**, 556-564, doi:10.1016/S1470-2045(06)70732-X (2006).

35 Ozdemir, N. O., Turk, N. S. & Duzcan, E. IMP3 expression in urothelial carcinomas of the urinary bladder. *Turk Patoloji Derg* **27**, 31-37, doi:10.5146/tjpath.2010.01044 (2011).

36 Sitnikova, L. *et al.* IMP3 predicts aggressive superficial urothelial carcinoma of the bladder. *Clin Cancer Res* **14**, 1701-1706, doi:10.1158/1078-0432.CCR-07-2039 (2008).

37 Yang, F., Zhou, Q., Meng, L. & Xing, N. IMP3 is a biomarker for non-muscle-invasive urothelial carcinoma of the bladder associated with an aggressive phenotype. *Medicine (Baltimore)* **98**, e16009, doi:10.1097/MD.0000000000016009 (2019).

38 Komor, A. C., Badran, A. H. & Liu, D. R. CRISPR-Based Technologies for the Manipulation of Eukaryotic Genomes. *Cell* **169**, 559, doi:10.1016/j.cell.2017.04.005 (2017).

39 Huang, Q. D. *et al.* IMP3 promotes TNBC stem cell property through miRNA-34a regulation. *Eur Rev Med Pharmacol Sci* **22**, 2688-2696, doi:10.26355/eurrev_201805_14965 (2018).

40 Zhao, W. *et al.* Insulin-like growth factor 2 mRNA binding protein 3 (IGF2BP3) promotes lung tumorigenesis via attenuating p53 stability. *Oncotarget* **8**, 93672-93687, doi:10.18632/oncotarget.21280 (2017).

41 You, S., Guan, Y. & Li, W. Epithelialmesenchymal transition in colorectal carcinoma cells is mediated by DEK/IMP3. *Mol Med Rep* **17**, 1065-1070, doi:10.3892/mmr.2017.7943 (2018).

42 Shida, D., Takabe, K., Kapitonov, D., Milstien, S. & Spiegel, S. Targeting SphK1 as a new strategy against cancer. *Curr Drug Targets* **9**, 662-673, doi:10.2174/138945008785132402 (2008).

43 Pyne, N. J. & Pyne, S. Sphingosine 1-phosphate and cancer. *Nat Rev Cancer* **10**, 489-503, doi:10.1038/nrc2875 (2010).

44 Maiti, A., Takabe, K. & Hait, N. C. Metastatic triple-negative breast cancer is dependent on SphKs/S1P signaling for growth and survival. *Cell Signal* **32**, 85-92, doi:10.1016/j.cellsig.2017.01.021 (2017).

45 Lommel, M. *et al.* Protein O-mannosylation is crucial for E-cadherin-mediated cell adhesion. *Proc Natl Acad Sci U S A* **110**, 21024-21029, doi:10.1073/pnas.1316753110 (2013).

46 Sorensen, K. M. *et al.* Upregulation of Mrps18a in breast cancer identified by selecting phage antibody libraries on breast tissue sections. *BMC Cancer* **17**, 19, doi:10.1186/s12885-016-2987-5 (2017).

Figures

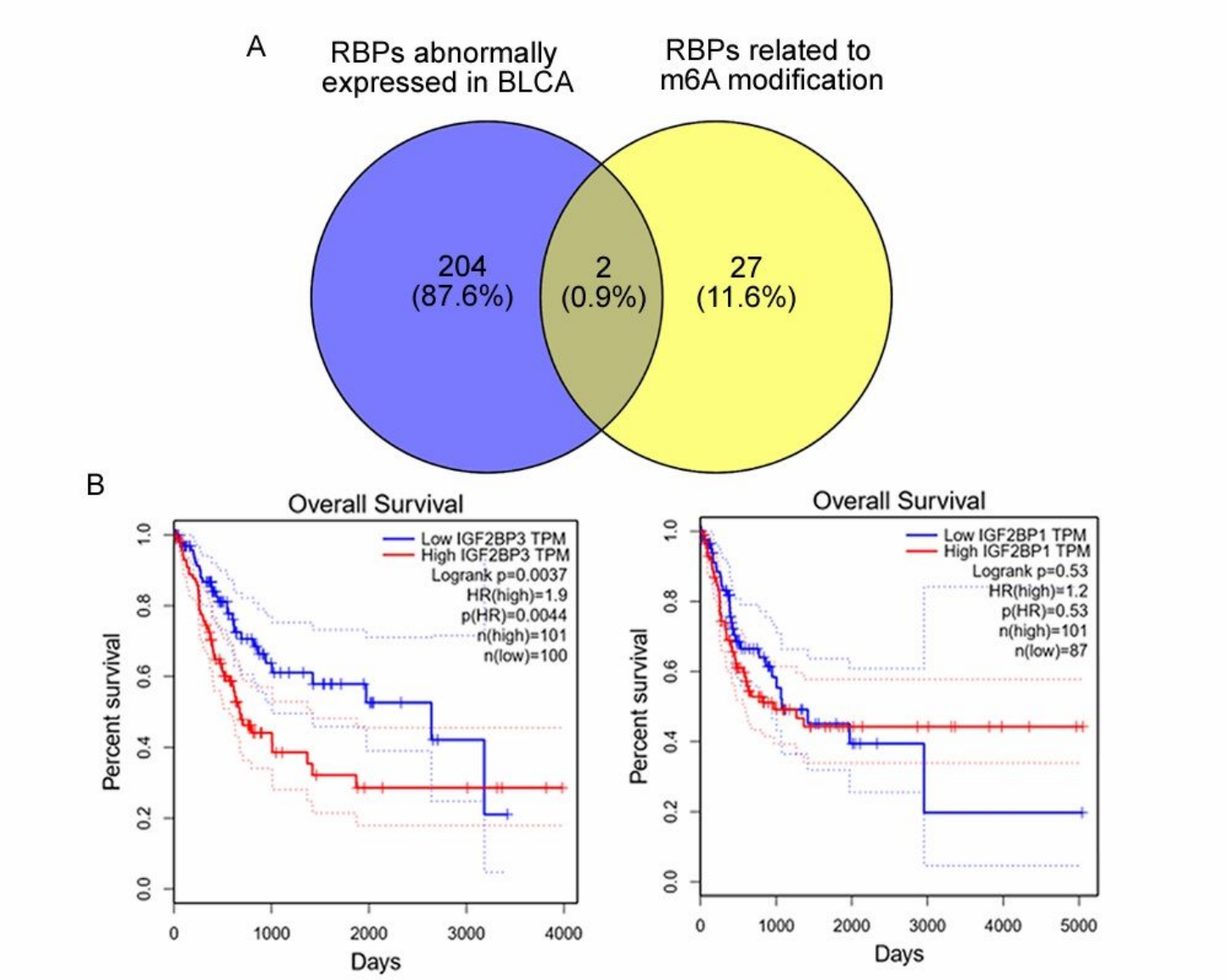

Figure 1

.

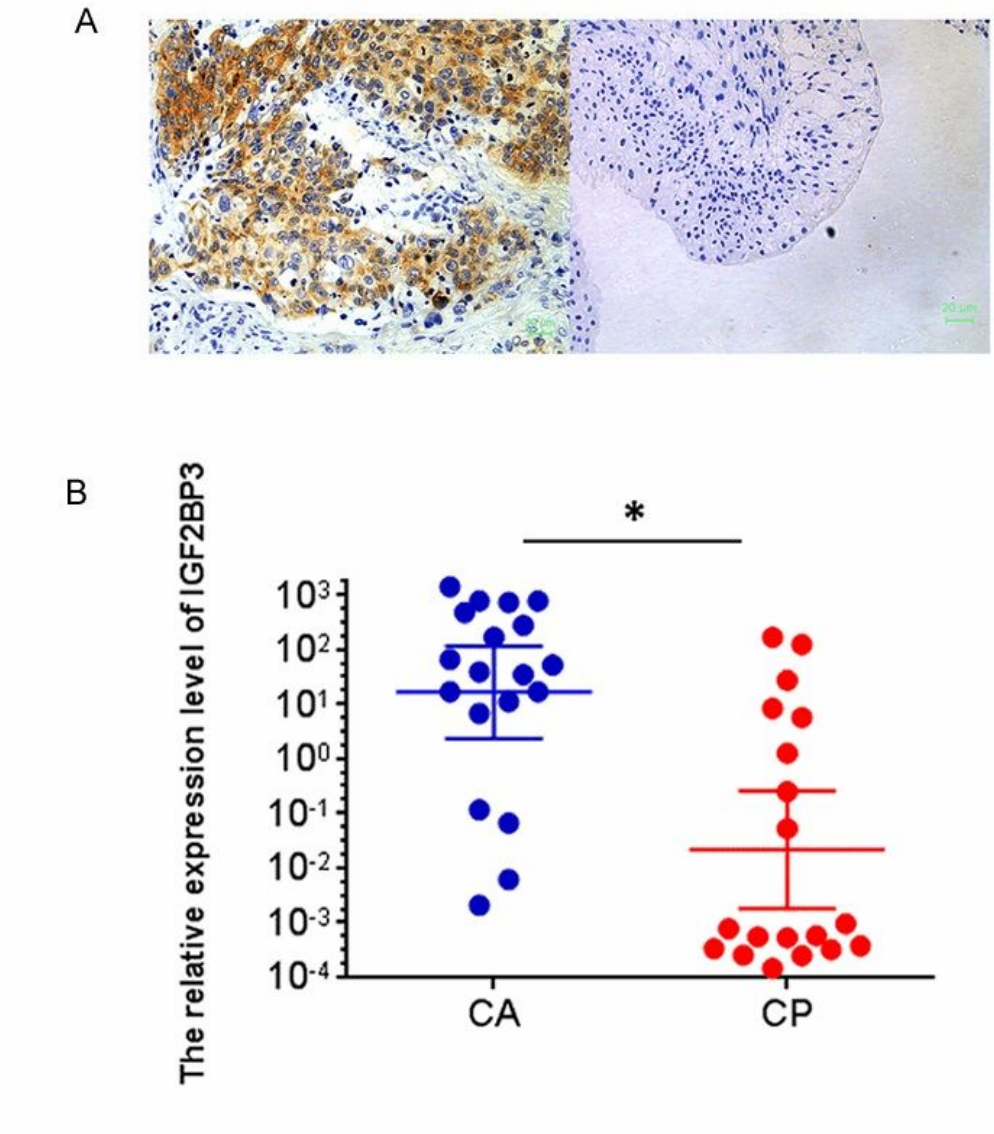
A
B
The relative expression level of IGF2BP3
*
10^3
10^2
10^1
10^0
10^{-1}
10^{-2}
10^{-3}
10^{-4}
CA
CP

Figure 2

.

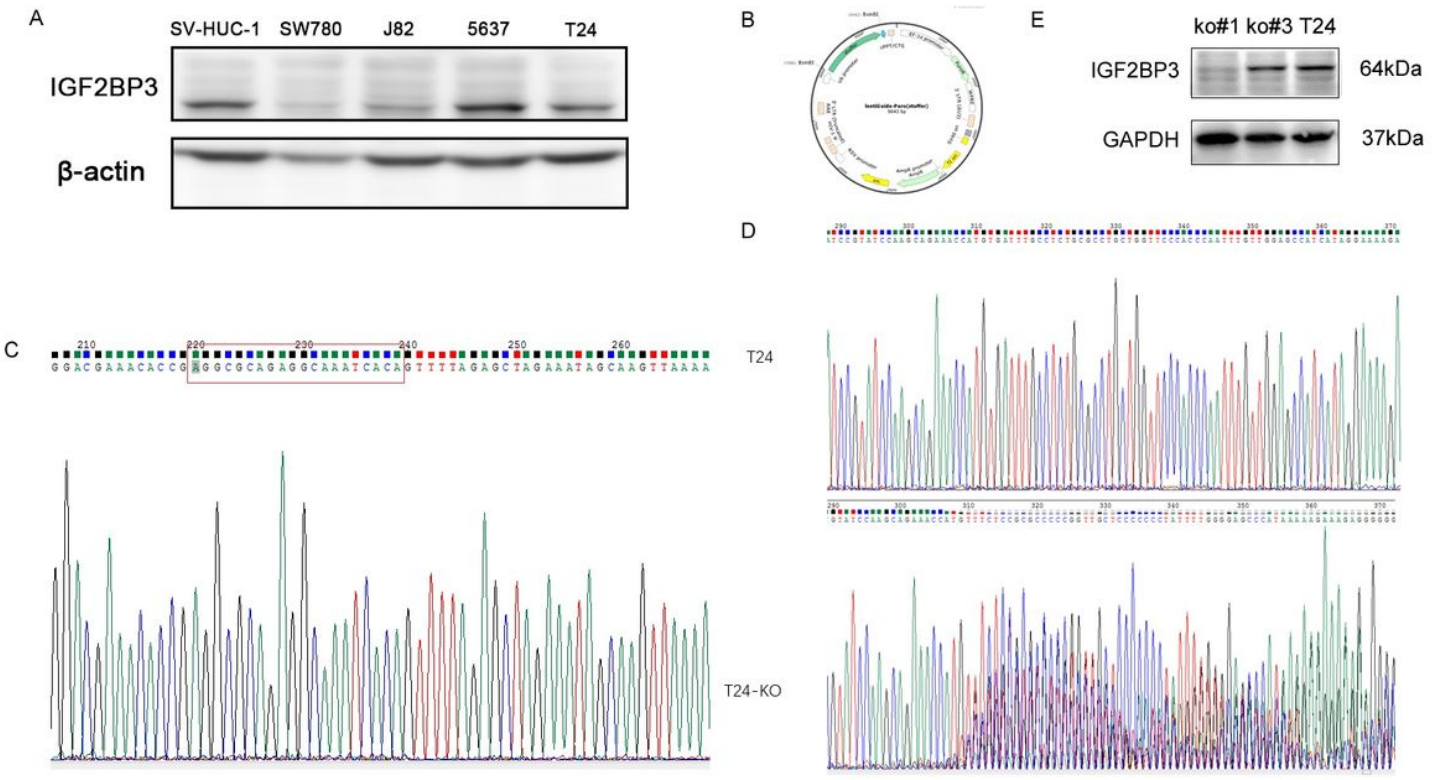
A
SV-HUC-1
SW780
J82
5637
T24
IGF2BP3
β-actin
B
E
ko#1 ko#3 T24
IGF2BP3
64kDa
GAPDH
37kDa
C
T24
T24-KO
D

Figure 3

.

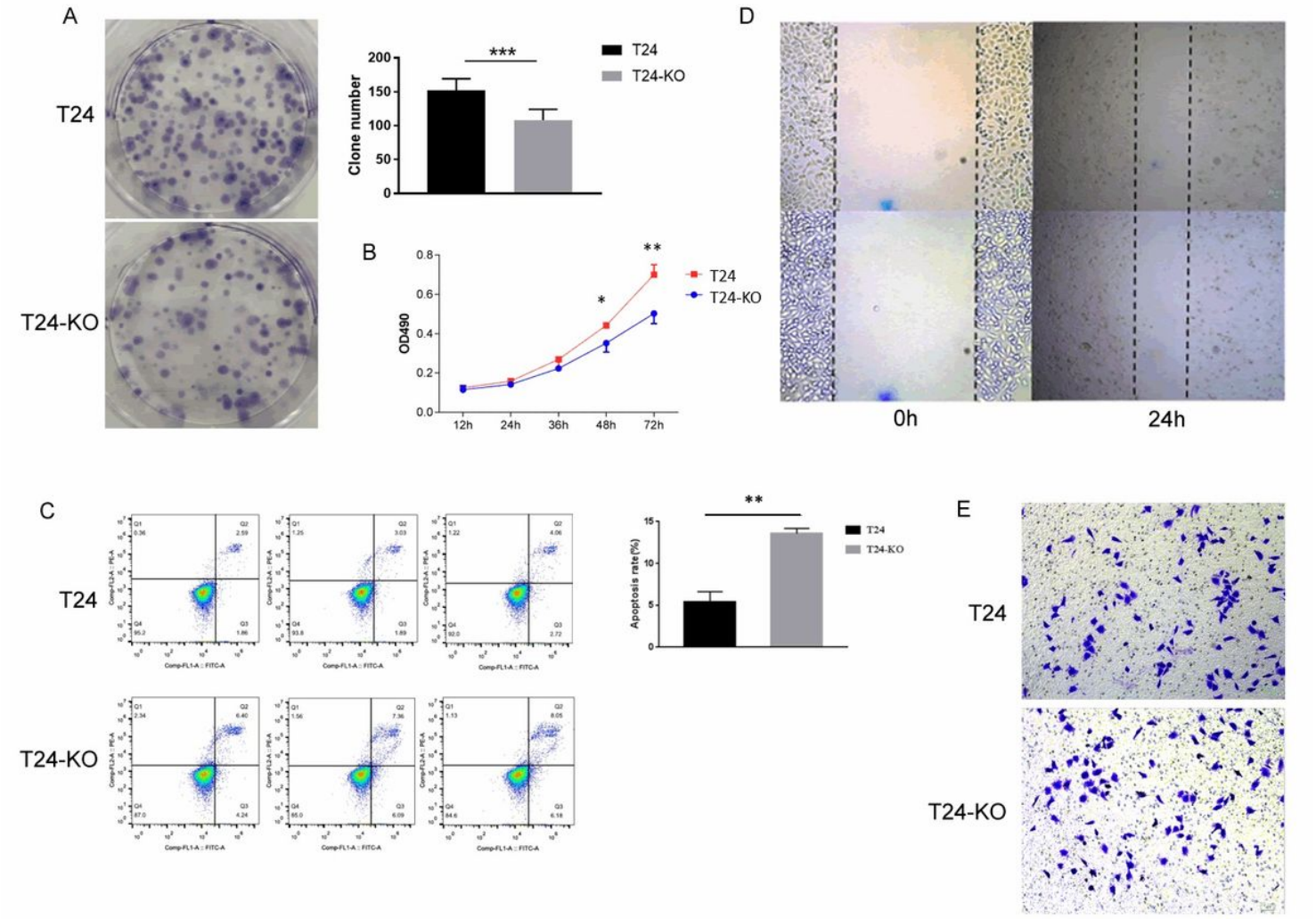

Figure 4

.

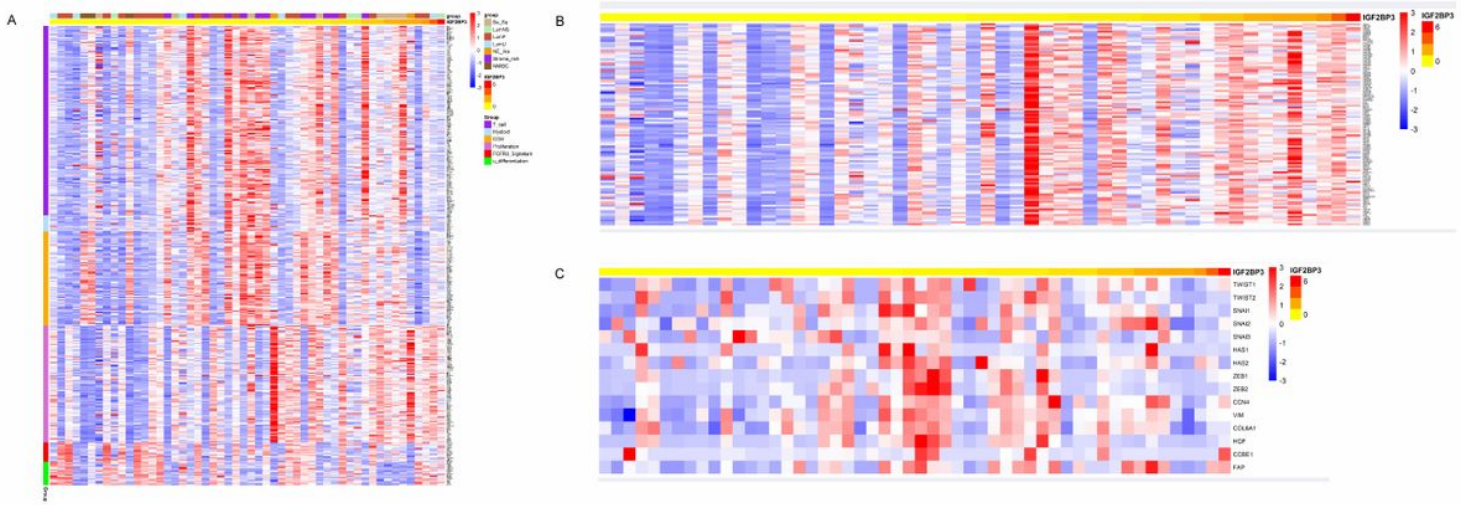

Figure 5

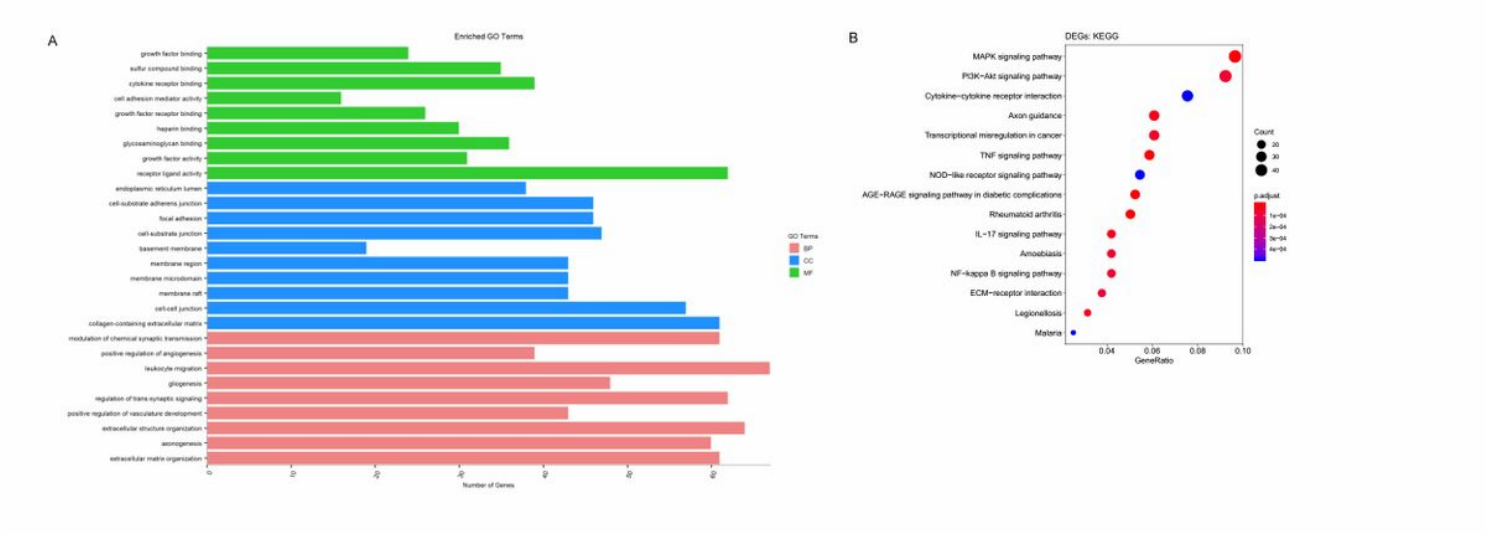

Figure 6

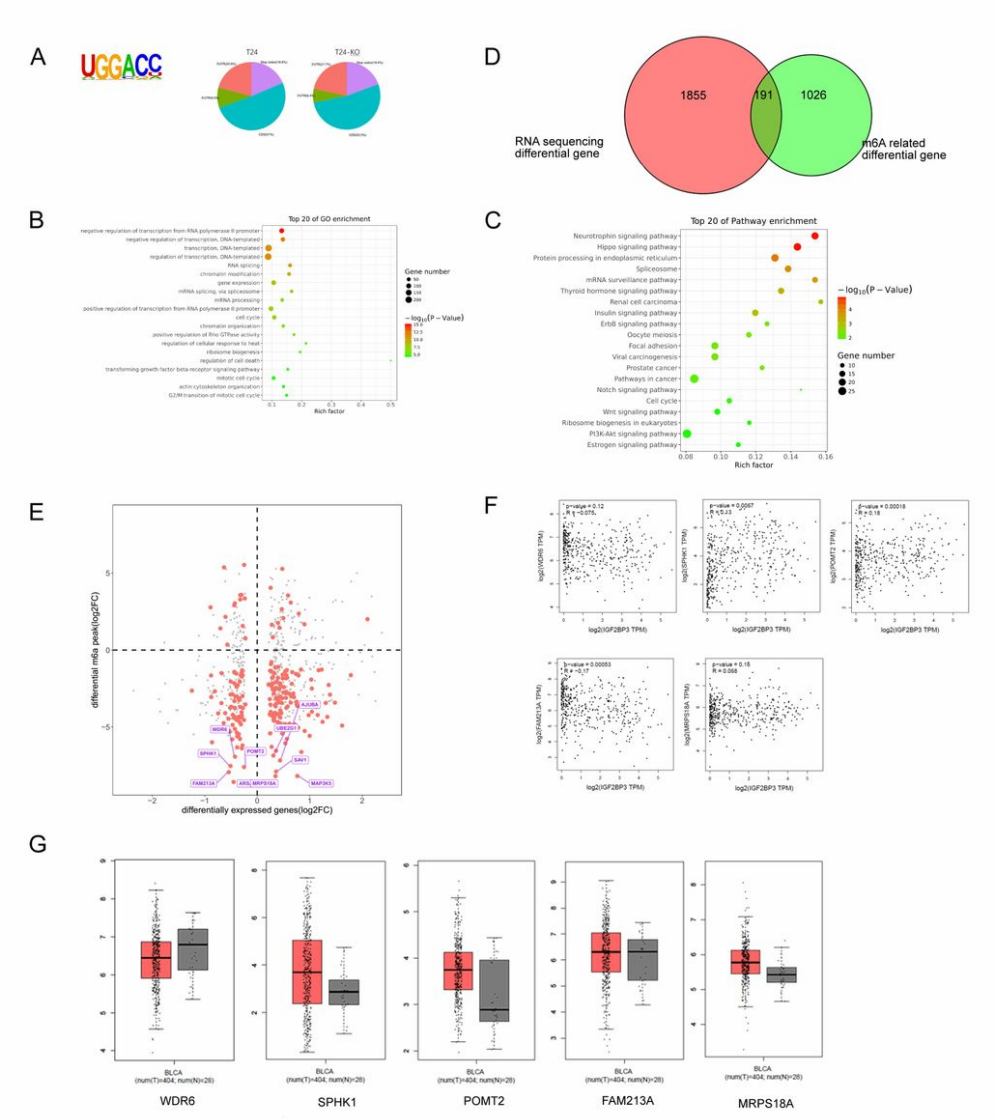

Figure 7

.